Proceedings of IMECE2002
ASME International Mechanical Engineering Congress & Exposition
November 17–22, 2002, New Orleans, Louisiana

IMECE2002-39487

STRESS ANALYSES AND STRUCTURAL MODIFICATIONS OF FABRIC COMPOSITE SEAMS

Wenzhong Tang and Michael Keefe
126 Spencer Lab, Mechanical Engineering Department, University of Delaware
Newark, Delaware 19716-3140, USA
302-831-8009, Fax 302-831-3619, keefe@me.udel.edu

ABSTRACT

An adhesively bonded seam is a common method of joining coated fabrics in the manufacturing of inflatables. In this paper, Nylon and Polyester seams are studied both experimentally and numerically. In the numerical analyses, the seam components are described with layered models containing fabric composite layers. The in-plane and out-of-plane elastic constants of the fabric composite layers are derived using the crimp model and a stacked model respectively. An existing finite element code, ANSYS 5.7 is used to perform two-dimensional stress analyses of the seams under tension. In the analyses, a stress concentration factor is defined to evaluate the strength of the seams in comparison with their base fabric laminates. Numerical data show that Nylon seams are almost as strong as their base laminate but there is strength degradation in Polyester seams, which agrees well with test results. Finally, two structural modifications are proposed to improve the strength of the Polyester seams. The modifications are evaluated by both simulations and tests.

Keywords: Coated Fabrics, Composites, Modeling, Stress Analysis

INTRODUCTION

Inflatables such as inflatable habitats, airships and aerostats are manufactured from flexible composite materials (coated fabrics) that are made structural via internal inflation pressure [1,2]. Inflatable composite structures may present significant benefits over conventional structures for many applications: higher strength to weight ratios, flexibility, and smaller launch or transport vehicles are some of the potential benefits.

Inflatables are made up of pieces of coated fabrics. One common method of joining coated fabrics is to use an adhesively bonded seam. A good seam should not be the weak link in a structure. Three common types of adhesively bonded seams in use are overlap seam, single tape seam, and double tape seam. In this paper, a Nylon double tape seam and a Polyester double tape seam are investigated.

Adhesively bonded joints under tension have been studied by many researchers using various methods [3-16]. Because the failure of the adhesive layer due to shear or peel is the predominant failure mode of adhesively bonded joints under tension, almost all the previous authors put their emphasis on the shear and peel stresses in the bond layer(s). However, as far as the Nylon and Polyester seams in this study are concerned, the bonding strength of the adhesives is so high that the failure of the base fabric laminates due to tension and bending turns out to be the only failure mode. Therefore, unlike earlier studies, the present work concentrates on the tensile stresses in the base fabric laminates. In this paper, a commercial finite element code, ANSYS 5.7, is used to perform two-dimensional finite element stress analyses of the seams.

NOMENCLATURE

$1, 2, 3$ = material axes of a lamina or a fabric composite layer
a = length of undulation
A_{ij} = averaged in-plane stiffness
$A_{ij}(x)$ = local in-plane stiffness
E = Young's modulus
G = shear modulus
h = thickness of a fabric composite layer
$h_1(x)$ = shape function of undulation
h_f = thickness of a fill lamina
h_w = thickness of a warp lamina
Q_{ij} = elastic stiffness matrix
t = thickness
V, Vol = volume fractions
x, y, z = Cartesian coordinates
$\theta(x)$ = local off-axis angle in fiber undulation
ν = Poisson's ratio

ε = strain
σ = stress
Δ = change
Superscripts and subscripts
W, w = quantities of a warp lamina or a warp fiber
F, f = quantities of a fill lamina or a fill fiber

SEAM CONFIGURATIONS AND MICROSTRUCTURES OF THE FABRIC LAMINATES

1.1 Seam configurations

The configurations of the seams are shown in Figure 1. In the Nylon double tape seam, the two pieces of Nylon base laminates are heat-bonded to two Nylon structural tapes having the same microstructure as the base laminates. In the Polyester double tape seam, the two pieces of Polyester base laminates are connected by a Polyester structural tape and a cover tape. The structural tape itself is a fabric laminate and heat-bonded to the Polyester base laminates on one side. The other side of the Polyester base laminates is bonded to the Tedlar cover tape using a layer of adhesive.

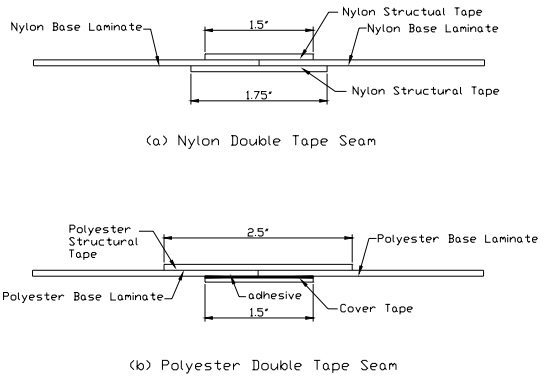

Figure 1 Seam Configurations.

1.2 Microstructures of the fabric laminates

In the seams, both the base laminates and the structural tapes are coated fabrics or fabric laminates.

The Nylon laminate consists of a plain weave Nylon fabric (210 Denier, 40×40 Count) coated with Polyether Urethane and Polycarbonate Polyurethane. In this paper, the laminate is considered as a continuum and a layered model is used to describe its microstructure as shown in Figure 2. In the model, the Polyether Urethane coatings go into the Nylon fabric and form a fabric composite layer. On each side of the composite layer is bonded a layer of Polycarbonate.

The Polyester base laminate consists of a layer of Tedlar film, a layer of Mylar film, a plain weave Polyester fabric (1000 Denier, 18×21 Count), and several adhesive layers. The layered model of the Polyester base laminate is illustrated in Figure 3. Urethane coatings go into the Polyester fabric and form a fabric composite layer.

The Polyester Structural Tape consists of a Polyester fabric (220×1000 Denier, 10×24 Count) coated with several adhesive layers. The layered model of the Polyester structural tape is illustrated in Figure 4. In the model, Polyether Polyurethane base coatings go into the Polyester fabric and form a fabric composite layer. On each side of the composite layer, a layer of Polyester urethane is coated.

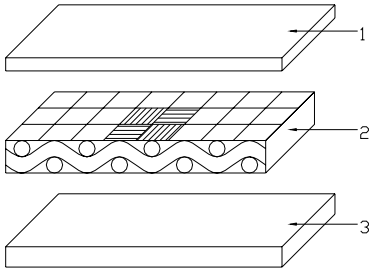

Figure 2 Layered Model of the Nylon Laminate: 1-Polycarbonate Polyurethane; 2-Fabric Composite Layer; 3-Polycarbonate Polyurethane.

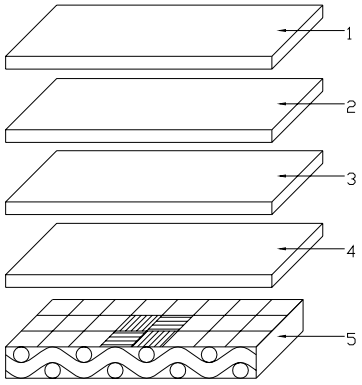

Figure 3 Layered Model of the Polyester Base Laminate 1-Tedlar Film; 2-Black Polyester Urethane Adhesive; 3- Mylar Film; 4- Black Polyester Urethane Adhesive; 5- Fabric Composite Layer.

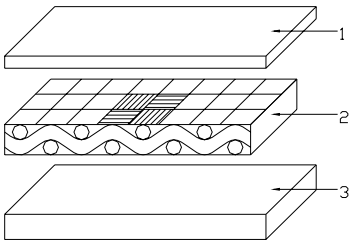

Figure 4 Layered Model of the Polyester Structural Tape 1-Polyether Urethane; 2- Fabric Composite Layer; 3- Polyether Urethane.

ELASTIC CONSTANTS OF THE FABRIC COMPOSITE LAYERS IN THE LAMINATES

2.1 Background

In the above layered models of the laminates, each model has a fabric composite layer. The effective elastic constants of the composite layers are needed in the stress analyses of the seams under tension. In the past 3 decades, many researchers have devoted their efforts to predicting the mechanical

properties of fabric composites from the known material properties of their constituent phases [17-26].

For simplicity, in this paper, the crimp model is used to derive the in-plane elastic constants of the composite layers and a stacked model is proposed for the out-of-plane elastic constants.

2.2 Crimp model for the in-plane elastic constants of a plain weave fabric composite

2.2.1 Crimp model

Figure 5 depicts the geometry of the crimp model for plain weave fabric composites where the warp yarn is allowed to be different from the filling yarn.

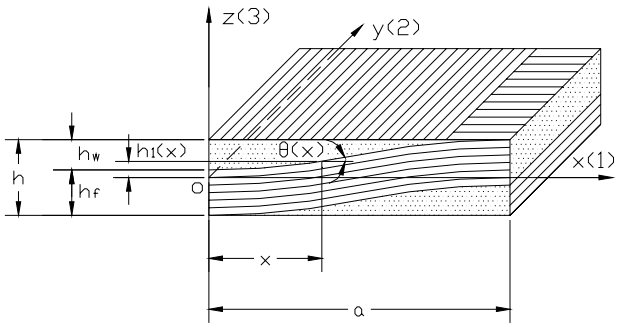

Figure 5 Crimp Model for Plain Weave Fabric Composites (After Ishikawa and Chou, 1983).

In the model, the undulation shape of the filling yarn is defined by the parameters $h_1(x)$, h, h_w, h_f and a. To simulation the actual configuration, the following form of crimp is assumed for the filling:

$$h_1(x) = \left\{1 + \sin\left[(x - \frac{a}{2})\frac{\pi}{a}\right]\right\}\frac{h_w}{2} + h_f - \frac{h}{2} \qquad (1)$$

It is assumed that the laminated plate theory is applicable to each infinitesimal piece of the model along the x axis. Thus, the local extensional stiffness A_{ij}'s are expressed as functions of x by

$$A_{ij}(x) = \int_{-h/2}^{h_1(x)-h_f} Q_{ij}^W dz + \int_{h_1(x)-h_f}^{h_1(x)} Q_{ij}^F(\theta) dz + \int_{h_1(x)}^{h/2} Q_{ij}^W dz$$
$$= h_w Q_{ij}^W + h_f Q_{ij}^F(\theta), \qquad (i,\ j = 1,\ 2,\ 6) \qquad (2)$$

where the superscripts W and F signify warp and filling yarn respectively. Q_{ij}^W is the stiffness of the warp yarn. $Q_{ij}^F(\theta)$ is the local stiffness of the filling yarn. The equations (2.14), (6.23) to (6.26) in Reference 19 are used to calculate Q_{ij}^W and $Q_{ij}^F(\theta)$. With local stiffness $A_{ij}(x)$, the average extensional stiffness can be defined as

$$A_{ij} = \frac{1}{a}\int_0^a A_{ij}(x) dx, \qquad (i,\ j = 1,\ 2,\ 6) \qquad (3)$$

In the present work, a numerical method is used to calculate these average quantities.

2.2.2 Relationships of equivalent in-plane elastic moduli (E_{11}, E_{22}), shear modulus (G_{12}), and Poisson's ratios (ν_{12}, ν_{21}) of plain weave fabric composites to their average extensional stiffness constants A_{11}, A_{22}, A_{12} and A_{66}

Macroscopically, a fabric composite layer can be assumed to be a homogeneously idealized orthotropic material, and thus does not account for the details of fiber-resin geometry and interaction. Consider a fabric composite layer of thickness h whose material axes (1, 2, 3) are aligned with its geometric axes (x, y, z), where 1 and 2 denote yarn directions and 3 the thickness direction. Based on the classical plate theory [27], we have

$$A_{11} = Q_{11}h,\ A_{22} = Q_{22}h,\ A_{12} = Q_{12}h,\ A_{66} = Q_{66}h \qquad (4)$$

and

$$Q_{11} = \frac{E_{11}}{(1 - \nu_{12}\nu_{21})}, \quad Q_{22} = \frac{E_{22}}{(1 - \nu_{12}\nu_{21})}$$

$$Q_{12} = \frac{\nu_{12}E_{22}}{(1 - \nu_{12}\nu_{21})}, \quad Q_{66} = G_{12} \qquad (5)$$

where Q_{11}, Q_{22}, Q_{12}, and Q_{66} are the stiffness matrix quantities of the homogeneous material. Thus,

$$\frac{A_{11}}{h} = \frac{E_{11}}{(1 - \nu_{12}\nu_{21})}, \quad \frac{A_{22}}{h} = \frac{E_{22}}{(1 - \nu_{12}\nu_{21})}$$
$$\frac{A_{12}}{h} = \frac{\nu_{12}E_{22}}{(1 - \nu_{12}\nu_{21})}, \quad \frac{A_{66}}{h} = G_{12} \qquad (6)$$

where

$$\frac{\nu_{12}}{E_{11}} = \frac{\nu_{21}}{E_{22}} \qquad (7)$$

From equations 6 and 7, the in-plane elastic constants of the fabric composite layer can be derived as

$$\nu_{xy} = \nu_{12} = \frac{A_{12}}{A_{22}}, \quad \nu_{yx} = \nu_{21} = \nu_{12}\frac{A_{22}}{A_{11}}$$
$$E_{xx} = E_{11} = \frac{A_{11}(1 - \nu_{12}\nu_{21})}{t}$$
$$E_{yy} = E_{22} = \frac{A_{22}(1 - \nu_{12}\nu_{21})}{h}$$
$$G_{xy} = G_{12} = \frac{A_{66}}{h} \qquad (8)$$

2.3 Stacked model for the out-of-plane elastic constants of a plain weave fabric composite

2.3.1 Stacked model

From the above crimp model, the in-plane moduli, shear modulus and Poisson's ratios of a fabric composite layer can be derived. To obtain its out-of-plane elastic modulus (E_{zz}), shear moduli (G_{xz}, G_{yz}), and Poisson's ratios (ν_{xz}, ν_{yz}), a stacked model, Figure 6, is considered.

In the model, a fabric composite layer is composed of two laminae, warp and fill, with one lamina stacked on the top of the other. The Young's moduli, shear moduli, and Poisson's

ratios of the warp and the fill laminae can be calculated from the material properties and volume fractions of their constituent phases [19].

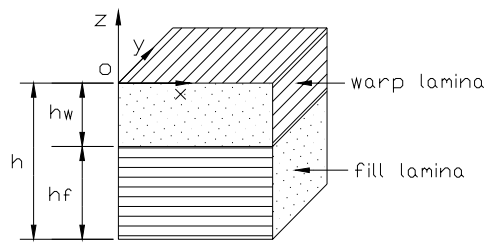

Figure 6 Stacked Models for a Fabric Composite Layer.

2.3.2 Young's modulus E_{zz}

Consider the deformation of the stacked model under a simple compression test in the z direction (compression stress = σ_z). After the deformation, the model takes its new thicknesses h', h'_w and h'_f as shown in Figure 7.

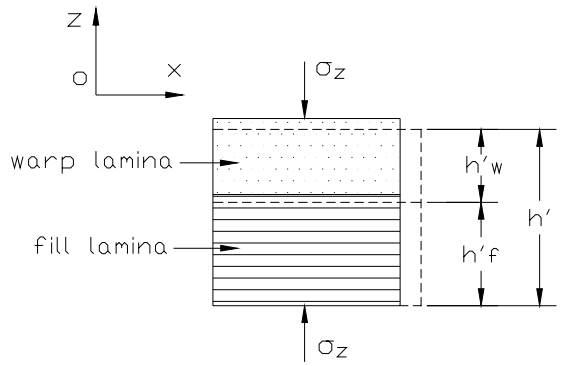

Figure 7 Deformation of the Stacked Model under a Simple Compression Test in the z Direction.

The size changes in the thickness direction are defined as

$$\Delta h = h' - h \,, \Delta h_w = h'_w - h_w \,, \Delta h_f = h'_f - h_f \qquad (9)$$

Thus, the resulted z direction strains of the fabric composite layer and the two laminae are

$$\varepsilon_z = \Delta h / h \,, \varepsilon_z^w = \Delta h_w / h_w \,, \varepsilon_z^f = \Delta h_f / h_f \qquad (10)$$

These strains can also be written as

$$\varepsilon_z = \sigma_z / E_{zz} \,, \varepsilon_z^w = \sigma_z / E_{zz}^w \,, \varepsilon_z^f = \sigma_z / E_{zz}^f \qquad (11)$$

where E_{zz}, E_{zz}^w and E_{zz}^f are the Young's modulus of the fabric composite layer, the warp lamina and the fill lamina respectively. Then, the strain of the composite layer can be derived from equations in (4.10) and (4.11).

$$\varepsilon_z = \frac{\Delta h}{h} = \frac{\Delta h_w + \Delta h_f}{h} = \frac{h_w \varepsilon_z^w}{h} + \frac{h_f \varepsilon_z^f}{h}$$
$$= \frac{h_w}{h}\frac{\sigma_z}{E_{zz}^w} + \frac{h_f}{h}\frac{\sigma_z}{E_{zz}^f} \qquad (12)$$

Thus the Young's modulus E_{zz} of the fabric composite layer can be calculated from the sizes and properties of the warp and the fill lamina as

$$E_{zz} = \frac{\sigma_z}{\varepsilon_z} = \frac{\sigma_z}{\frac{h_w}{h}\frac{\sigma_z}{E_{zz}^w} + \frac{h_f}{h}\frac{\sigma_z}{E_{zz}^f}} = \frac{1}{\frac{h_w}{h}\frac{1}{E_{zz}^w} + \frac{h_f}{h}\frac{1}{E_{zz}^f}} \qquad (13)$$

2.3.3 Poisson's ratios ν_{xz} *and* ν_{yz}

Consider the deformation of the stacked model under a simple tensile test in the x direction (Fig. 8).

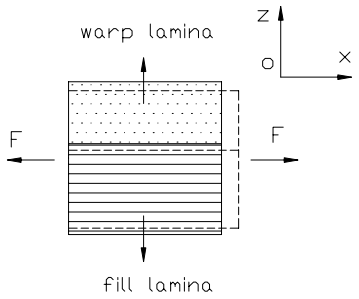

Figure. 8 Deformation of the Stacked Model under a Simple Tensile Test in the x direction.

Assume both the warp and the fill lamina have the same strain ε_x in the load direction. In the z direction, the strains are assumed to be ε_z^w and ε_z^f for the warp and fill lamina respectively. Thus

$$\nu_{xz}^w = -\frac{\varepsilon_z^w}{\varepsilon_x} \,, \nu_{xz}^f = -\frac{\varepsilon_z^f}{\varepsilon_x} \qquad (14)$$

Using equation (12), the Poisson's ratio ν_{xz} of the fabric composite layer can be calculated as

$$\nu_{xz} = -\frac{\varepsilon_z}{\varepsilon_x} = -\frac{\frac{h_w \varepsilon_z^w}{h} + \frac{h_f \varepsilon_z^f}{h}}{\varepsilon_x}$$
$$= -\left(\frac{h_w}{h}\frac{\varepsilon_z^w}{\varepsilon_x} + \frac{h_f}{h}\frac{\varepsilon_z^f}{\varepsilon_x}\right) = \frac{h_w}{h}\nu_{xz}^w + \frac{h_f}{h}\nu_{xz}^f \qquad (15)$$

Similarly, the ν_{yz} of the fabric composite layer can be calculated as

$$\nu_{yz} = \frac{h_w}{h}\nu_{yz}^w + \frac{h_f}{h}\nu_{yz}^f \qquad (16)$$

2.3.4 Shear moduli G_{xz} *and* G_{yz}

Using the Rule of Mixtures [27], the shear moduli G_{xz} and G_{yz} of the fabric composite layer are calculated as

$$\frac{1}{G_{yz}} = \frac{Vol_w}{G^w_{yz}} + \frac{Vol_f}{G^f_{yz}} = \frac{h_w}{h}\frac{1}{G^w_{yz}} + \frac{h_f}{h}\frac{1}{G^f_{yz}}$$
$$\frac{1}{G_{xz}} = \frac{Vol_w}{G^w_{xz}} + \frac{Vol_f}{G^f_{xz}} = \frac{h_w}{h}\frac{1}{G^w_{xz}} + \frac{h_f}{h}\frac{1}{G^f_{xz}} \quad (17)$$

where Vol_w and Vol_f are the volume fractions of the warp and the fill lamina in the fabric composite layer respectively.

2.4 Elastic constants of the fabric composite layers in the fabric laminates

2.4.1 Elastic constants of the fabric composite layer in the Nylon laminate

Table 1 lists the elastic properties of all the component materials. All the components are assumed to be isotropic. The Poisson's ratios of the polymeric adhesives are assumed to be 0.4.

Table 2 lists the elastic properties and volume fractions of the Nylon fiber and the matrix in the laminae of the composite layer. In this case, the warp lamina has the same properties as the fill lamina. With equations (2.2) through (2.6) in Reference 19, the elastic constants of the laminae are calculated Then the crimp and the stacked models are used to derive the 3-D elastic constants of the Nylon composite layer and listed in Table 3, where x and y signify the yarn directions and z the thickness direction.

Table 1 Properties of the Component Materials in the Nylon Laminate

Product Description	Density (g/cm^3)	Young's Modulus (MPa)	Poisson's Ratio
Polycarbonate Polyurethane	1.21	25.5	0.4
Polyether Urethane	1.135	7.929	0.4
Nylon Fabric, Plain Weave,210 Denier, 40 Count	1.14	4229	0.41
Tedlar Film	1.46	2103	0.4
Black Polyester Urethane Adhesive	1.21	8.274	0.4
Clear 0.5 Mil Mylar Film	1.39	5003	0.38
Black Aliphatic Urethane Adhesive	1.07	3.447	0.4
Polyester Fabric, Plain Weave 1000 Denier, 18×21 Count	1.38	6710	0.4
Black Aromatic Urethane Adhesive	1.13	7.584	0.4
Polyether Polyurethane Base Coat, Black	1.004	2.413	0.4
Polyester Fabric, Plain Weave, 220×1000 Denier, 10×24 Count	1.380	220 Denier: 7465 1000 Denier: 6710	0.4

Table 2 Elastic Constants and Volume Fractions of the Fiber and the Matrix in the Warp/Fill Lamina of the Nylon Composite Layer

	Fiber (Nylon)	Matrix (Polyether Urethane)
Equivalent Thickness (mm)	$t_f = 0.03347$	$t_m = 0.02988$
Volume Fraction	$V_f = 0.528$	$V_m = 0.472$
Young's Modulus (MPa)	$E_f = 4229$	$E_m = 7.929$
Poisson's Ratio	$\nu_f = 0.41$	$\nu_m = 0.4$

Table 3 Three Dimensional Elastic Constants of the Fabric Composite Layer in the Nylon Laminate

Young's Moduli (MPa)	Shear Moduli (MPa)	Poisson's Ratios
$E_{xx} = 1115.5$	$G_{xy} = 9.136$	$\nu_{xy} = 0.01386$
$E_{yy} = 1115.5$	$G_{yz} = 10.82$	$\nu_{yz} = 0.3407$
$E_{zz} = 31.95$	$G_{xz} = 10.82$	$\nu_{xz} = 0.3407$

2.4.2 Elastic constants of the fabric composite layer in the Polyester base laminate

The Polyester fabric has the same yarn but different yarn counts in the warp and the fill directions (21×18 Count). Table 4 lists the elastic properties and volume fractions of the Polyester fiber and the matrix in the laminae of the composite layer. Here, the fill and warp laminae have different properties due to their different yarn counts. It is reasonable to assume that the two laminae have the same thickness. The matrix is assumed to be the mixture of the Aliphatic Urethane and the Aromatic Urethane, and its Young's modulus is calculated by volume average.

Table 4 Elastic Constants and Volume Fractions of the Fiber and the Matrix in the Warp/Fill Lamina of the Composite Layer in the Polyester Base Laminate

	Fiber (Polyester)	Matrix (Aliphatic/Aromatic Urethane)
Equivalent Thickness (mm)	18 count direction: $t_f = 0.06$ 21 count direction: $t_f = 0.07$	18 count direction: $t_m = 0.022$ 21 count direction: $t_m = 0.012$
Volume Fraction	18 count direction: $V_f = 0.732$ 21 count direction: $V_f = 0.854$	18 count direction: $V_m = 0.268$ 21 count direction: $V_m = 0.146$
Young's Modulus (MPa)	$E_f = 6710$	$E_m = 5.271$
Poisson's Ratio	$\nu_f = 0.4$	$\nu_m = 0.4$

The elastic constants of the laminae are calculated and then the 3-D elastic constants of the whole composite layer are calculated and listed in Tables 5, where x and y signify the 18 and 21 count yarn directions respectively and z the thickness direction.

Table 5 Three Dimensional Elastic Constants of the Fabric Composite Layer in the Polyester Base Laminate

Young's Moduli (MPa)	Shear Moduli (MPa)	Poisson's Ratios
$E_{xx} = 2482.4$	$G_{xy} = 17.92$	$\nu_{xy} = 0.01013$
$E_{yy} = 2881.2$	$G_{yz} = 21.14$	$\nu_{yz} = 0.2886$
$E_{zz} = 59.72$	$G_{xz} = 18.50$	$\nu_{xz} = 0.2676$

2.4.3 Elastic constants of the fabric composite layer in the Polyester structural tape

The fabric in the Polyester structural tape has different yarns as well as different yarn counts in the warp and the fill directions (220×1000 Denier, 10×24 Count). The elastic constants and volume fractions of the fiber and the matrix in the two laminae of the composite layer are listed in Table 6. The elastic constants of the laminae are calculated and then the 3-D elastic constants of the whole composite layer are calculated and listed in Table 7, where x and y signify the 24 and 10 count yarn directions respectively and z the thickness direction.

Table 6 Elastic Constants and Volume Fractions of the Fiber and the Matrix in the Laminae of the Fabric Composite Layer in the Polyester Structural Tape

	Fiber (Polyester)	Matrix (Polyether Polyurethane)
Equivalent Thickness (mm)	10 count direction: $t_f = 0.007837$ 24 count direction: $t_f = 0.08549$	10 count direction: $t_m = 0.03380$ 24 count direction: $t_m = 0.03380$
Volume Fraction	10 count direction: $V_f = 0.188$ 24 count direction: $V_f = 0.717$	10 count direction: $V_m = 0.812$ 24 count direction: $V_m = 0.283$
Young's Modulus (MPa)	10 count direction: $E_f = 7465$ 24 count direction: $E_f = 6710$	$E_m = 2.413$
Poisson's Ratio	$\nu_f = 0.4$	$\nu_m = 0.4$

TENSILE TESTS

To compare the strength of the seams with that of their base laminates, tensile tests of both the base laminates and the seams were run on an Instru-Met machine. The tests were based on the ASTM Standard Test Method D5035-95 for Breaking Force and Elongation of Textile Fabrics [28]. This test method is also recommended for the determination of the breaking force and elongation of coated fabrics. According to the standard, the tests were run with specimen width = 2 inches, gauge length = 6 inches, and test speed = 50 mm/min.

Table 7 Three Dimensional Elastic Constants of the Fabric Composite Layer in the Polyester Structural Tape

Young's Moduli (MPa)	Shear Moduli (MPa)	Poisson's Ratios
$E_{xx} = 3571.9$	$G_{xy} = 4.196$	$\nu_{xy} = 0.01893$
$E_{yy} = 367.6$	$G_{yz} = 3.381$	$\nu_{yz} = 0.2386$
$E_{zz} = 9.453$	$G_{xz} = 2.943$	$\nu_{xz} = 0.4164$

Table 8 Breaking Forces (N) of the Base Laminates and the Seams

	Number Of Samples	Average Breaking Force (N)	Maximum Breaking Force (N)	Minimum Breaking Force (N)
Nylon Base Laminate	12	1208.8	1302.39	1037.79
Nylon Double Tape Seam	30	1250.5	1348.96	1116.44
Polyester Base Laminate	4	2787.3	2948.82	2622.67
Polyester Double Tape Seam	42	2389.1	2650.76	1931.89

3.1 Breaking forces

The breaking forces for the base laminates and the seams are listed in Table 8. It is obvious that there is no noticeable strength degradation in the Nylon seams whereas the Polyester double tape seam is about 14.3% weaker than its base laminate.

3.2 Statistics of failure zones

3.2.1 Nylon double tape seam

Figure 9 shows the zone partition of the Nylon double tape seam sample. In all the 30 samples tested, none broke in the bonded seam region, 12 samples broke in the seam edge zone (1), 10 in the heat treated zone (2), 3 in the heat treated edge zone (3), and 5 in outer laminate zone (4).

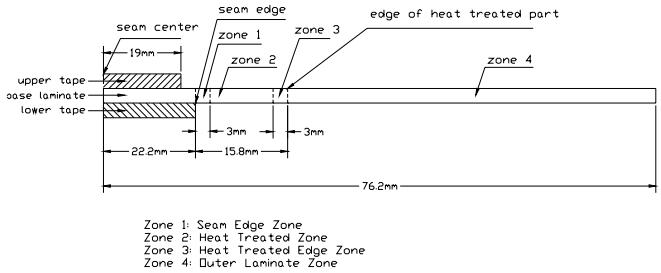

Figure 9 Zone Partition of the Nylon Double Tape Seam Sample.

3.2.2 Polyester double tape seam

Figure 10 shows the zone partition of the Polyester double tape seam sample. The sample is divided into seam zone and outer laminate zone. In all the 42 samples tested, none broke in the seam zone, 41 broke right at the seam edge, and1 in the outer laminate zone.

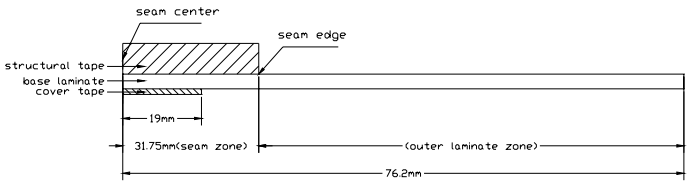

Figure 10 Zone Partition of the Polyester Double Tape Seam Sample.

FINITE ELEMENT ANALYSES OF THE SEAMS UNDER TENSION

4.1 Nylon double tape seam

4.1.1 Geometric model, mesh and boundary conditions

Due to its symmetry in structure, only half the length of the Nylon double tape seam sample needs to be considered in the finite element analysis. Its geometric model is shown in Figure 11. The base laminate and the structural tapes have layered structures. The material properties of the layers are listed in Table 1 and 3.

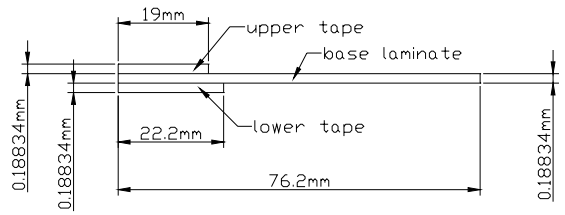

Figure 11 Geometric Model of the Nylon Double Tape Seam Sample.

The finite element mesh used Plane42 2-D structural solid element. Finer meshes are used around the edge of the wider tape to obtain converged tensile stresses in this region. The symmetry displacement boundary conditions are applied to the left end nodes only on the tapes and the right end nodes are fixed in the thickness direction but applied a displacement of desired extension in the length direction.

4.1.2 Simulation results

Under extension, the maximum tensile stress occurs at a bottom-row node in the composite layer of the base laminate at a very small distance (<0.1 mm) from the edge of the lower tape. Figure 12 gives the tensile stresses for the bottom row nodes in composite layer of the base laminate when the extension is 0.762 mm (1%). The maximum and average tensile stresses are marked on the graph, by which the stress concentration factor can be calculated.

As Figure 15 shows, the stress concentration factor of the Nylon double tape seam seems to approach 1 at large extension. The Nylon double tape seam samples are as strong as the base laminate and break at a random location outside the bonded part.

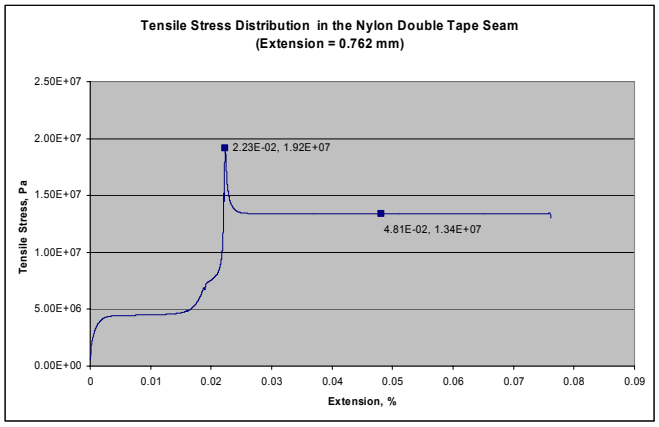

Figure 12 Tensile Stress Distributions in the Nylon Double Tape Seam.

4.2 Polyester double tape seam

4.2.1 Geometric model, mesh and boundary conditions

Similar to the Nylon double tape seam, only half the length of the Polyester double tape seam sample needs to be considered in the finite element analysis. Its geometric model is shown in Figure 13. The base laminate and the structural tapes have layered structures. The material properties of the layers are listed in Tables 1and 5.

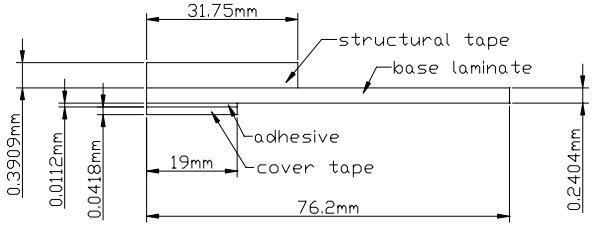

Figure 13 Geometric Model of the Polyester Double Tape Seam Sample.

The finite element mesh again used Plane42 2-D structural solid element. Finer meshes are used around the edge of the structural tape to obtain converged tensile stresses in this area. The symmetry displacement boundary conditions are applied to the left end nodes only on the tapes and the right end nodes are fixed in the thickness direction but applied a displacement of desired extension in the length direction.

4.2.2 Simulation results

Under extension, the maximum tensile stress in the composite layer of the base laminate occurs at the top-row node at the edge of the structural tape. Figure 14 gives the tensile stresses for the top row nodes in composite layer of the base laminate when the extension is 0.762 mm (1%). The maximum and average tensile stresses are marked on the graph, by which the stress concentration factor can be calculated.

Figure 15 gives the stress concentration factor of the Nylon and Polyester double tape seam at different extension. The extension in the graph goes up to 1.15%. Simulations at larger extensions were unsuccessful due to small equation solver pivot items and error in element formulation. Unlike the Nylon double tape seam, the stress concentration factor of the

Polyester double tape seam decreases slowly with extension and shows a different qualitative shape.

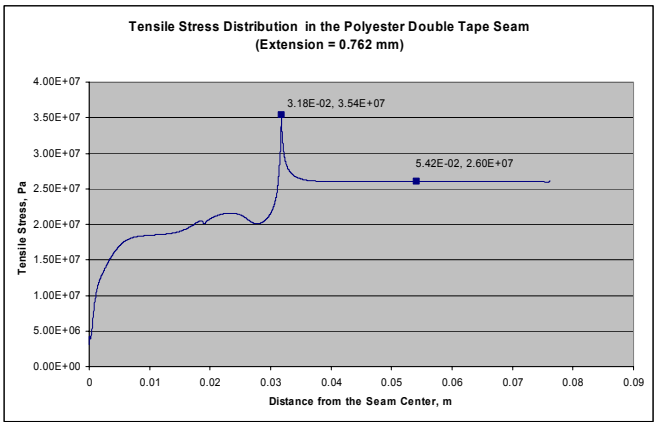

Figure 14 Tensile Stress Distribution in the Polyester Double Tape Seam.

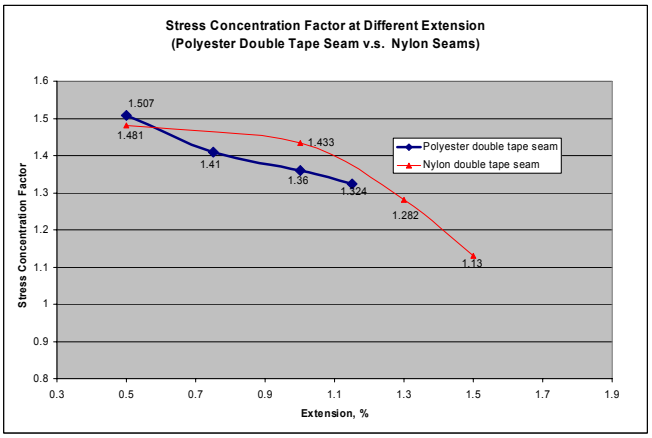

Figure 15 Stress Concentration Factor of the Polyester Double Tape Seam.

Structural modifications of the Polyester double tape seam

The tensile strength of a seam is, to some extent, determined by its stress concentration factor. The lower the stress concentration factor of a seam, the closer its strength is to that of its base laminate. Previous simulation results hint that the stress concentration factor of the Polyester double tape seam would stay high at large extension, which could explain why there is noticeable strength degradation in this specific seam structure. One possible way to improve the seam strength is to bring down the stress concentration factor. In this section, two structural modifications are proposed. One is to extend the width of the cover tape (from 1.5 to 4 inch total width), and the other is to replace the polyester structural tape with the Nylon structural tape used in the Nylon double tape seam. Extending the cover tape mitigates the stiffness and geometry discontinuity at the edge of the structural tape whereas replacing Polyester with Nylon structural tape reduces the stiffness discontinuity by replacing with a more extensible material. One is primarily a 'geometry' change whereas the other is primarily a material property change.

5.1 Simulation of the modified Polyester double tape seams

Similar finite element analyses were performed on the modified Polyester double tape seams.

Figure 16 gives the stress concentration factor of the modified seams at different extension. The results of the original Nylon and Polyester double tape seams are also provided in the graph for comparison. The stress concentration factor of the nylon structural tape modified seam is tending to go below that of the original seam at large extension. Therefore, the breaking force of that modified seam is expected to be higher than the original seam.

It is obvious that the stress concentration factor is also reduced by the wider cover tape modification. Thus, the seam strength can be expected to be improved. However, unlike the previous material modification, this geometric modification does not affect the shape of the response.

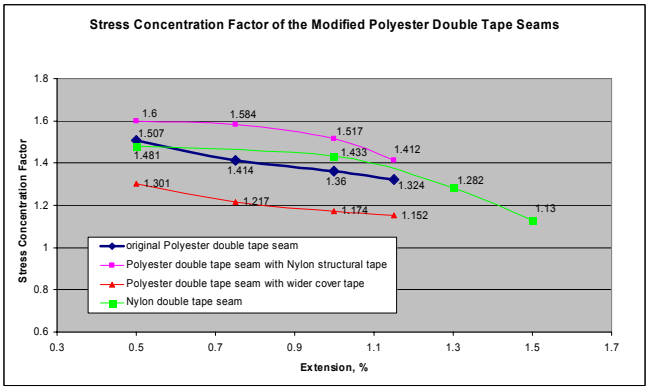

Figure 16 Stress Concentration Factor of the Modified Polyester Double Tape Seam with Nylon Structural Tape.

5.2 Test results

The modified structures were then made and tested. The tensile test results are listed in Table 9. Thus both modifications improved the seam strength. Replacing the Polyester structural tape with the Nylon structural tape improves the seam strength from 85.7% to 93.9% of the strength of the base laminate, while using a wider cover tape improves the seam strength to 90.8% of the strength of the base laminate.

Table 9 Breaking Strength of the Modified Polyester Double Tape Seams

	Base Laminate	Original Seam	Modified Seam #1	Modified Seam #2
Breaking Strength (N/Yarn Count)	75.33	64.57	70.70	68.36
Percentage of the Base Laminate Strength	100%	85.7%	93.9%	90.8%

#1- Modified seam with Nylon structural tape;
#2- Modified seam with wider cover tape.

Conclusion

Two dimensional stress analyses of a Nylon double tape seam and a Polyester double tape seam are performed using the existing finite element code, ANSYS 5.7. The microstructures of the fabric laminates are described by layered models. For the fabric composite layers in these layered models, the crimp model is used to derive their in-plane elastic constants, and a stacked model for their out-of-plane elastic properties. In the analyses, a stress concentration factor is defined to evaluate the tensile strengths of the seams in comparison with their base laminates.

Simulation results show that the stress concentration factors in the Nylon seam approaches unity as extension increases. The seams are expected to be as strong as their base laminate which agrees with test results. Unlike the Nylon seam, the stress concentration factor in the Polyester double tape seam stays relatively high as extension increases. This explains the strength degradation in the Polyester double tape seam and why almost all the Polyester seam samples broke at the location of the stress concentration.

Finally, two structural modifications are proposed to improve the strength of the Polyester double tape seam. The material modification, replacing the Polyester structural tape with a Nylon structural tape, improves the seam strength from 85.7% to 93.9% of the strength of its base laminate. The geometric modification, using a wider cover tape, improves the seam strength to 90.8% of the strength of base laminate.

ACKNOWLEDGMENTS

The authors gratefully acknowledge support for this work from the ILC Dover, Inc.

REFERENCES

[1] Cadogan, D., Grahne, M., and Mikulas, M., 1988, "Inflatable Space Structures: A New Paradigm for Space Structure Design," *49th International Astronautical Congress, Sept 28 - Oct 2, Melbourne, Astralia*.

[2] Cadogan, D., Stein, J., and Grahne, M., 1988, "Inflatable Composite Habitat Structures for Lunar and Mars Exploration." *49th International Astronautical Congress, Sept 28 - Oct 2, Melbourne, Astralia*.

[3] Goland, M., and Reissner, E., 1944, "The Stresses in Cemented Joints," ASME Journal of Applied Mechanics, **7**, A17-27.

[4] Hart-Smith, L.J., 1973, "Adhesive-Bonded Single-Lap Joints," Technical Report NASA CR-112236.

[5] Oplinger, D.W., 1994, "Effects of Adherend Deflections in Single Lap Joints," International Journal of Solids and Structures, **31**, pp. 2565-2587.

[6] Wooley, G.R., and Carver, D.R., 1971, "Stress Concentration Factors for Bonded Lap Joints," Journal of Aircraft, **8**, pp. 817-820.

[7] Reddy, J.N., and Roy, S., 1988, "Non-Linear Analysis of Adhesively Bonded Joints," International Journal of Non-Linear Mechanics, **23**, pp. 97-112.

[8] Bigwood, D.A., and Crocombe, A.D., 1990, "Non-Linear Adhesive Bonded Joint Design Analyses," International Journal of Adhesion and Adhesives, **10**, pp. 31-41.

[9] Pandey, P.C., Shankaragouda, H., and Singh, Arbind Kr., 1999, "Nonlinear Analysis of Adhesively Bonded Lap Joints Considering Viscoplasticity in Adhesives," Computers and Structures, **70**, pp. 387-413.

[10] Renton, W.J., and Vinson, J.R., 1977, "Analysis of Adhesively Bonded Joints between Panels of Composite Materials," ASME Journal of Applied Mechanics, **44**, pp. 101-106.

[11] Yang, C., and Pang, S.S., 1996, "Stress-Strain Analysis of Single-Lap Composite Joints under Tension," Journal of Engineering Materials and Technology, **118**, pp. 247-255.

[12] Tsai, M.Y., Morton, J., and Matthews, F.L., 1995, "Experimental and Numerical Studies of a Laminated Composite Single-Lap Adhesive Joint," Journal of Composite Materials, **29**, pp. 1554-1575.

[13] Li, G., Lee-Sullivan P., and Thring, R.W., 1999, "Nonlinear Finite Element Analysis of Stress and Strain Distributions across the Adhesive Thickness in Composite Single-Lap Joints," Composite Structures, **46**, pp. 395-403.

[14] Tong, L., Sheppard, A. and Kelly, D., 1995, "Relationship between Surface Displacement and Adhesive Peel Stress in Bonded Double Lap Joints," International Journal of Adhesion and Adhesives, **15**, pp. 43-48.

[15] Tong, L., Sheppard, A. and Kelly, D., 1996, "The Effect of Adherend Alignment on the Behavior of Adhesively Bonded Double Lap Joints," International Journal of Adhesion and Adhesives, **16**, pp. 241-247.

[16] Albat, A.M., and Romilly, D.P., 1999, "A Direct Linear-Elastic Analysis of Double Symmetric Bonded Joints and Reinforcements," Composites Science and Technology, **59**, pp. 1127-1137.

[17] Ishikawa, T., and Chou, T.-W., 1982, "Stiffness and Strength Behavior of Woven Fabric Composites," Journal of Materials Science, **17**, pp. 3211-3220.

[18] Ishikawa, T., and Chou, T.-W., 1983, "One-Dimensional Micromechanical Analysis of Woven Fabric Composites," AIAA Journal, **21**, pp. 1714-1721.

[19] Chou, T.-W., 1992, *Microstructural Design of Fiber Composites*, Cambridge University Press.

[20] Ramnath, V., 1985, "Elastic Properties of Woven Fabric Reinforced Composites," *A Collection of Technical Papers – AIAA/ASME/ASCE/AHS Structures, Structural Dynamics & Materials Conference*, pp. 420-425.

[21] Pastore, C.M., amd Gowayed, Y.A., 1994, "A Self-Consistent Fabric Geometry Model: Modification and Application of a Fabric Geometry Model to Predict the Elastic Properties of Textile Composites," Journal of Composites Technology & Research, **16**, pp. 32-36.

[22] Whitcomb, J.D., 1991, "Three-Dimensional Stress Analysis of Plain Weave Composites," *Composite Materials: Fatigue and Fracture (Third Volume), ASTM STP 1110*, T.K. O'Brien, Ed., American Society for Testing and Materials, Philadephia, pp. 417-438

[23] Aitharaju, V.R., and Averill, R.C., 1999, "Three-Dimensional Properties of Woven Fabric Composites," Composites Science and Technology, **59**, pp. 1901-1911.

[24] Kelkar, A.D., Shenoy, S., Whitcomb, J., and Tang, X., 2001, "Behavior of Plain woven Textile Composites Subjected to Uniaxial Tensile Loading," *A Collection of Technical Papers – AIAA/ASME/ASCE/AHS/ASC Structures, Structural Dynamics & Materials Conference*. Pp. 2443-2453.

[25] Carvelli, V., and Poggi, C. A., 2001, "Homogenization Procedure for the Numerical Analysis of Woven Fabric Composites," Composites, Part A, **32**, pp. 1425-1432.

[26] Ivanov, I., and Tabiei, A., 2001, "Three-Dimensional Computational Micro-Mechanical Model for Woven Fabric Composites," Composite Structures, **54**, pp. 489-496.

[27] Vinson, J.R., 1990, *The Behavior of Structures Composed of Composed Materials*, Kluwer Academic Publishers, Dordrecht.

[28] American Society for Testing and Materials, Annual Book of ASTM Standards, 1998, Vol.07.02, pp. 667-673.